

Displacement Control Strategies of an In-Line Axial-Piston Unit

L. Viktor Larsson and Petter Krus

Division of Fluid and Mechatronic Systems, Department of Management and Engineering
Linköping University, Linköping, Sweden
E-mail: viktor.larsson@liu.se, petter.krus@liu.se

Abstract

The need for efficient propulsion in heavy vehicles has led to an increased interest in hybrid solutions. Hydraulic hybrids rely on variable hydraulic pumps/motors to continuously convert between hydraulic and mechanical power. This process is carried out via the implementation of secondary control which, in turn, is dependent on a fast displacement controller response. This paper reports on a study of a prototype axial piston pump of the in-line type, in which the displacement is measured with a sensor and controlled using a software-based controller. A pole placement control approach is used, in which a simple model of the pump is used to parametrise the controller using desired resonance and damping of the closed loop controller as input. The controller's performance is tested in simulations and hardware tests on the prototype unit. The results show that the pole placement approach combined with a lead-compensator controller architecture is flexible, easy to implement and is able to deliver a fast response with high damping. The results will in the future be used in further research on full-vehicle control of heavy hydraulic hybrids.

Keywords: Hydraulic hybrids, displacement control, pole placement

1 Introduction

Increased oil prices and environmental concerns are driving research on energy efficient solutions for propulsion of heavy construction machines. One solution that has recently attracted great interest is hybridisation. This concept involves a combination of an internal combustion engine and a rechargeable energy storage device, and may yield energy savings for example by down-sizing the engine and incorporating energy recuperation [1]. In hydraulic hybrids, the energy storage device is a hydraulic accumulator which stores energy in compressed gas [2]. In turn, this energy-storing process relies on efficient variable pumps/motors that may transfer power between the hydraulic and the mechanical domains [3].

The inclusion of an accumulator in a hydraulic circuit causes the system pressure to be constant, or *impressed* [4] by the accumulator's state-of-charge. As a consequence, the controlled variable of a pump/motor connected to an accumulator is the shaft torque via the variable pump/motor displacement. This concept is central to hydraulic hybrid vehicles and is commonly referred to as *secondary control*. Secondary control in turn implies specific demands on variable displacement control, such as rapid response and the ability to realise negative displacement [5].

For safety reasons, it is usually desired to implement a cascaded control strategy, in which the displacement controller constitutes the innermost loop [6]. The response of the displacement controller should therefore be as fast as possible

compared to the outer loop. In addition, in multiple-mode power-split hydraulic hybrids, too slow displacement actuators cause drops in vehicle output torque during the mode shift [7]. The response requirements depend on properties such as maximum displacement, system pressure and experienced inertia, as well as the control strategy applied in the outer loop [4]. Numerical values of the requirements are therefore difficult to give without a specific application, but to manage the mode shifts the authors found that a swivel time (time from 0 to maximum displacement) below approximately 0.2-0.3 seconds was necessary for a medium-sized (9000 kg) construction machine [7].

Different pump/motor types fulfil the demands on displacement controllers to different degrees. This paper concerns swash-plate axial-piston units as they are considered a suitable compromise between efficiency and displacement controllability. In swash-plate pumps/motors, changing the swash-plate angle varies the displacement. This action may be realised by different actuating systems which may be mechanical, electro-mechanic, hydraulic or electro-hydraulic. Of the four types, actuators that use hydraulics are preferable for fast response [8].

Some research has been done on displacement control in swash-plate pumps/motors with hydraulic actuation, e.g. [6, 9–11]. However, [6] and [10] focus on 4-way servo-valve solutions. Moreover, Manring [11] considers a system with mechanical feedback which means that the valve dynamics

may be ignored [12]. In an early publication, Green et al. [9] compare 4-way valve and 3-way valve solutions, but do not consider units connected to accumulators.

This paper studies control strategies for a hydraulic, 3-way proportional valve actuator solution for displacement control in an axial-piston pump of swash-plate design connected to a circuit with an accumulator. Control concepts considered are proportional control and proportional-lead control. These concepts are parametrised with a pole placement approach, in which the desired resonance and damping of the closed-loop system are used as input.

The control strategies were tested and compared qualitatively and quantitatively in computer simulations and hardware tests on a prototype pump.

1.1 Delimitations

The effect of an accumulator in the circuit is studied to the extent that the system pressure is seen as impressed. Quantitative comparisons with a system without accumulator, or the effect of accumulator properties (size, pre-charge pressure etc.) on the system behaviour are not carried out. Furthermore, the pump/motor shaft dynamics' influence on the displacement controller is not considered in this paper.

2 Bosch A11VO Prototype Pump

The axial-piston, swash-plate unit studied in this paper is shown in fig. 1. It is a Bosh Rexroth A11VO prototype pump with a maximum displacement of 110 cm³/revolution. It has a maximum allowed operating pressure of 350 bar and a maximum allowed shaft rotational speed of 2800 rpm. The A11VO unit is intended to be used for secondary control in hybrid applications, and therefore one modification compared to its previous version is the ability to realise negative displacement. The particular unit studied in this paper, however, is equipped with a valve plate optimised for pump operation. All the tests have therefore been carried out with positive direction of the shaft.



Figure 1: Bosch A11VO pump studied in the paper.

2.1 Displacement Actuator

The displacement actuator circuit of the A11VO pump is shown in fig. 2. A proportional spool valve (1) controls the flow to the control piston (2) that acts on the swash plate (3), thereby changing the displacement angle, α . The proportional valve (1) is actuated with a solenoid that is fed with a

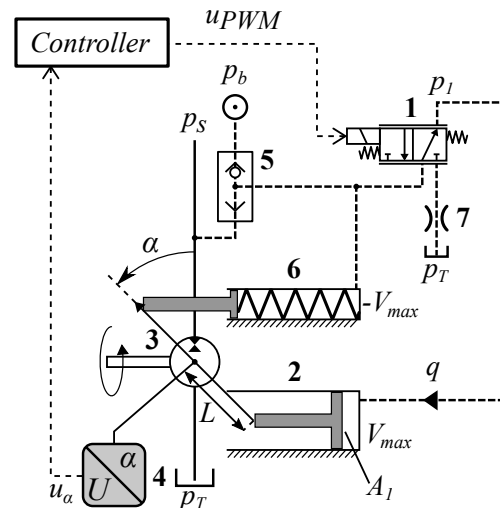


Figure 2: Controller mechanism in the A11VO pump.

pulse-width-modulated (PWM) voltage signal, u_{PWM} . An orifice (7) is mounted at the valve tank port for extra damping of the control mechanism. The displacement angle is measured with a Hall-effect sensor (4) and sent to an external controller for closed-loop control of the displacement.

The supply pressure to the valve (1) is either an external boost pressure, p_b , or the system pressure, p_s , managed by the shuttle valve (5). Here, p_b is assumed to be used only during start-up and that $p_s > p_b$ during normal operation of the pump. Furthermore, a spring-loaded piston (6), supplied with the same pressure as the valve (1), acts on the swash-plate (3) in the opposite direction compared to the control piston (2). The spring forces the pump into maximum displacement in the case of insufficient supply pressure to the valve (1). This feature is useful in a pump, as it allows for pressure to build up from start-up by the pump itself.

In a secondary controlled transmission, the spring forcing the unit into maximum displacement could be dangerous as it would result in maximum unit output torque, thus accelerating the vehicle. In future versions of the A11VO, it might therefore be necessary to change the start-up displacement configuration. This could for example be done by adding a spring acting on the control piston, thereby centering the displacement to zero [8]. The unstable nature of secondary controlled systems could imply further issues related to the displacement controller, such as in the event of a control valve power-outage. These issues are outside the scope of this paper, but should be considered in a final design.

3 Model

A model of the displacement actuator has previously been developed by the authors. In this paper, the same model is used for controller design and evaluation. For the controller design, a linearised representation is used, while the full model used for evaluation contains several non-linearities. The model's features of main importance are presented in this section. See [13] for further details concerning the model.

3.1 Linearised Representation

The linearised open-loop system is modelled as:

$$\Delta \varepsilon = G_O(s) \cdot \Delta u_{PWM} = \frac{K_s}{s \left(\frac{s}{\omega_v} + 1 \right)} \cdot \Delta u_{PWM} \quad (1)$$

where the input is the PWM voltage, Δu_{PWM} , and the output is the relative displacement, $\Delta \varepsilon$. ω_v is the valve break frequency that lumps the valve spool and solenoid dynamics. K_s is the lumped system gain:

$$K_s = \frac{k_{PWM} K_q}{A_1 L \alpha_{max}} \quad (2)$$

where α_{max} is the maximum swash plate angle, A_1 is the pressurised area of the control piston ((2) in fig. 2), and L is the distance from the swash plate's centre of rotation to the contact point of the control piston. k_{PWM} is the static gain from PWM duty cycle to valve spool position. K_q is the valve flow gain, calculated at a linearisation point ($p_{s,0}$, $p_{1,0}$, $p_{T,0}$):

$$K_q = -\frac{\partial q}{\partial x_v} = \begin{cases} C_q d \pi \sqrt{\frac{2}{\rho} (p_{1,0} - p_{T,0})}, & x_v \geq 0 \\ C_q d \pi \sqrt{\frac{2}{\rho} (p_{s,0} - p_{1,0})}, & x_v < 0 \end{cases} \quad (3)$$

where p_1 is the pressure in the control piston chamber, C_q is the valve flow coefficient, x_v is the valve displacement, ρ is the oil density and d is the valve spool diameter. Since the pump is assumed to be connected to an accumulator, the system pressure, p_s , is viewed as constant from a control perspective. The tank pressure, p_T , is assumed negligible compared to the other pressures. The damping orifice (7 in fig. 2) is lumped in the valve model.

3.2 Non-linearities

The full model is implemented in Hopsan, a system simulation tool developed at Linköping University [14]. An overview of the model structure is shown in fig. 3. As can be seen, the rotational motion is translated to a translational one, and the mechanism is viewed as a 3-way valve controlled piston.

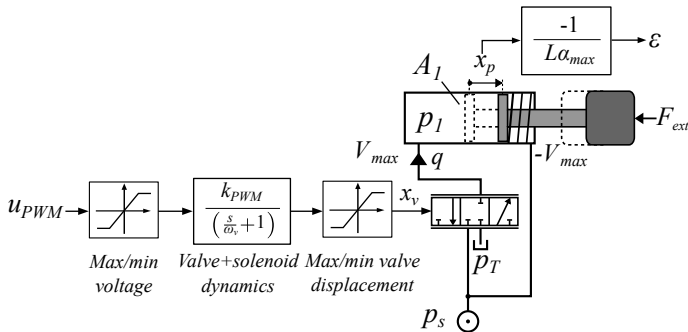


Figure 3: Schematic overview of Hopsan model.

Apart from the non-linearity of pressure-dependent flow gain shown in eq. (3), other relevant non-linearities included in the Hopsan model are:

- Saturation in valve stroke.
- Saturation in PWM voltage due to current limitations.
- Mean value of a speed- and pressure-dependant self-adjusting torque acting on the swash plate (F_{ext} in fig. 3).

The two first items act on the input signal of the system, as illustrated in fig. 3, while the self adjusting force is implemented as an external force, F_{ext} , that acts on the piston.

4 Control

The pure integrator in G_O requires a feedback loop for stabilisation. The controller is implemented as shown in fig. 4.

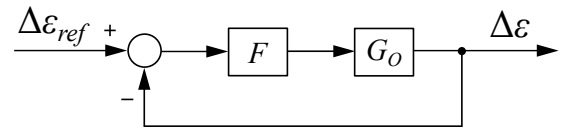


Figure 4: System (G_O , from eq. (1)) with controller (F) and feedback loop.

Two candidates for F are studied. The first candidate is a standard proportional controller (P):

$$F = K \quad (4)$$

The second candidate is a proportional controller with lead compensator (P-lead):

$$F = K \frac{\frac{s}{\omega_1} + 1}{\frac{s}{\omega_2} + 1} \quad (5)$$

None of the candidates contain purely integrating elements. This is motivated partly by the existence of a pure integrator in G_O , and partly by a desire to avoid problems caused by integrator wind-up when the controller is used as an inner loop in a full system. In other words, some static error is considered tolerable since it will be handled by an outer loop.

Compared to the P-lead controller, the P-controller has the advantages of simpler implementation and lower complexity. On the other hand, the P-lead controller offers higher flexibility and potentially higher performance than the P-controller. The achieved performance, however, depends on how K , ω_1 and ω_2 are chosen. That is, how the controller is parametrised.

4.1 Parametrisation: Pole Placement

With pole placement, the controller is parametrised by placing the poles of the closed-loop system according to given requirements [15]. The location of these poles depends on the system, which means that a system model is needed in the controller design for accurate results. Here, it is assumed that the input from the controller designer is desired resonance, ω_a , and relative damping, δ_a , of the closed loop system:

$$G_C = \frac{F \cdot G_O}{1 + F \cdot G_O} = \frac{1}{\frac{s^2}{\omega_v^2} + \frac{2\delta_a}{\omega_a} s + 1} \quad (6)$$

4.1.1 P-controller

Equations (1) and (4) with identification of ω_a and δ_a in eq. (6) yields that the controller gain, K , in the P-controller may be chosen as:

$$K = \frac{1}{\omega_v K_s} \omega_a^2 \quad (7)$$

or

$$K = \frac{\omega_v}{4K_s} \frac{1}{\delta_a^2} \quad (8)$$

Equations (7) and (8) show the limited flexibility of a proportional controller, as the controller gain is determined either by desired resonance or desired damping. It can be shown that for the P-controller:

$$\omega_a \delta_a = \frac{\omega_v}{2} \quad (9)$$

With a P-controller there is thus a compromise between damping and resonance (i.e. response), and to increase both of them simultaneously, a faster valve is required.

4.1.2 P-lead-controller

Equations (1) and (5) with identification of ω_a and δ_a in eq. (6) yields that ω_1 in the P-lead-controller may be chosen as:

$$\omega_1 = \omega_v \quad (10)$$

ω_2 may be chosen as:

$$\omega_2 = 2\omega_a \delta_a \quad (11)$$

The controller gain, K , may be chosen as:

$$K = \frac{\omega_a}{2K_s \delta_a} \quad (12)$$

With the P-lead-controller, the damping and resonance are decoupled, and may therefore be chosen independently of each other. Equation (10) means that there is a pole cancellation of the valve dynamics. With an ω_2 significantly higher than ω_v , a significantly faster response with maintained damping is therefore possible with the P-lead-controller compared to the P-controller. By transforming K and ω_2 into ω_a and δ_a , this response may in turn be trimmed in an intuitive and simple way.

4.2 Choosing ω_a and δ_a

As seen in section 4.1, ω_a and δ_a are achieved if the open loop system gain, K_s , and the valve break frequency, ω_v , are known. If this is the case, the P-controller could be designed either by choosing ω_a and accepting the resulting δ_a or vice

versa. With the P-lead-controller on the other hand, ω_a and δ_a may be chosen arbitrarily. This situation, however, is not entirely realistic, primarily for two reasons:

1. K_s and ω_v are subjects to system operating point- and day-to-day-variations.
2. Hardware limitations do not allow for infinitely fast response.

4.2.1 Parameter Variations

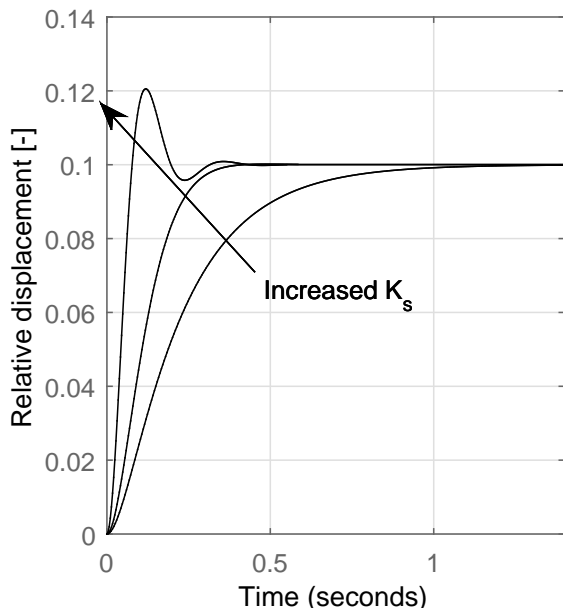
Figures 5 - 7 show how the system behaviour changes if K_s and ω_v deviate from the values with which the controller was designed. The plots have been generated with the linear model in eq. (1). The P-controller is parametrised with eq. (8) with $\delta_a = 0.9$. The P-lead-controller is parametrised with eqs. (10)-(12) with $\omega_a = 90$ rad/s and $\delta_a = 0.9$, which have been found to be suitable values in experiments. Both controllers are parametrised for $K_{s0} = 0.72$ and $\omega_{v0} = 26.6$ rad/s, which are estimates for a shaft speed of 1000 rpm and a system pressure of 200 bar.

As can be seen in figs. 5a and 5b, an increase in K_s with a P-controller decreases the phase margin, with a less damped response and higher resonance frequency as a result. The same principal behaviour is present with the P-lead-controller, which is why those corresponding graphs are not included in this section.

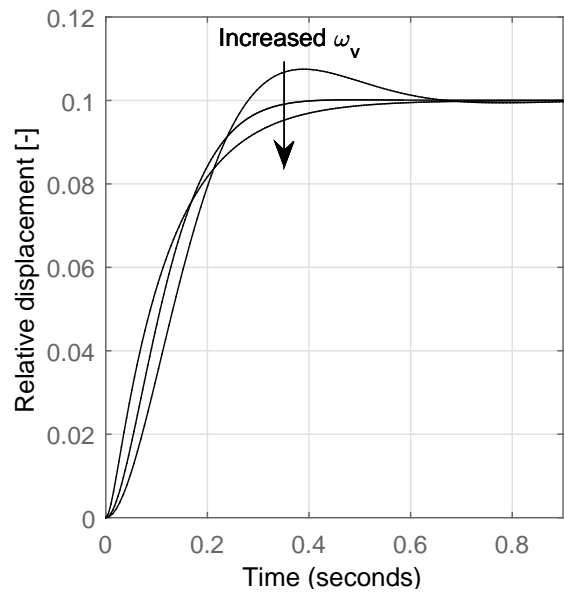
In contrast to K_s , an increase in ω_v increases the phase margin with a P-controller, as shown in fig. 6b. As seen in fig. 6a, this leads to a better damped response. With the P-lead-controller, fig. 7, a faster valve also increases the phase margin. However, if $\omega_1 \neq \omega_v$, the resulting closed loop is no longer of purely second order, as seen in fig. 7a.

From the discussion above, it may be concluded that from a stability point of view, the most critical point is when the system gain is at its highest and the valve break frequency its lowest. In a conservative approach, ω_a and δ_a should therefore be chosen at this point, with acceptance of slow performance in the other operating points. However, the dominance of low-order dynamics in the system makes it robust in the sense that it can tolerate quite large deviations in parameter values without reaching instability (the phase shift is always less than 180 degrees). The controller may therefore be trimmed at a point of interest and still be stable when deviating from this point, as long as changes in behaviour are tolerated. If too much oscillation occurs, the controller is then easily trimmed by increasing δ_a . Here, it is important to note that the linear model is simplified and does not, for example, include the hydraulic resonance or time delays in the software. These are factors that add phase shift and could become relevant if the system gain increases too much.

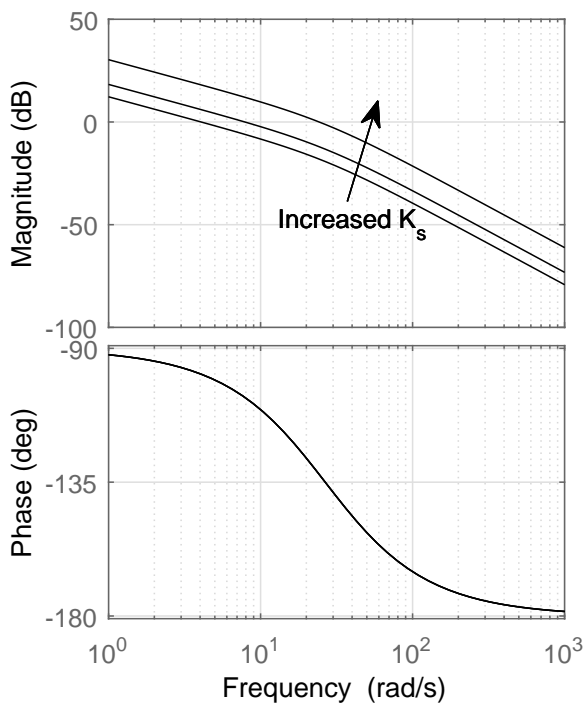
In this system, K_s has been observed to be the parameter that changes the most. The major reason for this is the change in the valve flow gain, K_q . As seen in eq. (3), this parameter changes with the pressure drop over the valve, which in turn depends on the system pressure, p_{s0} and the static pressure in



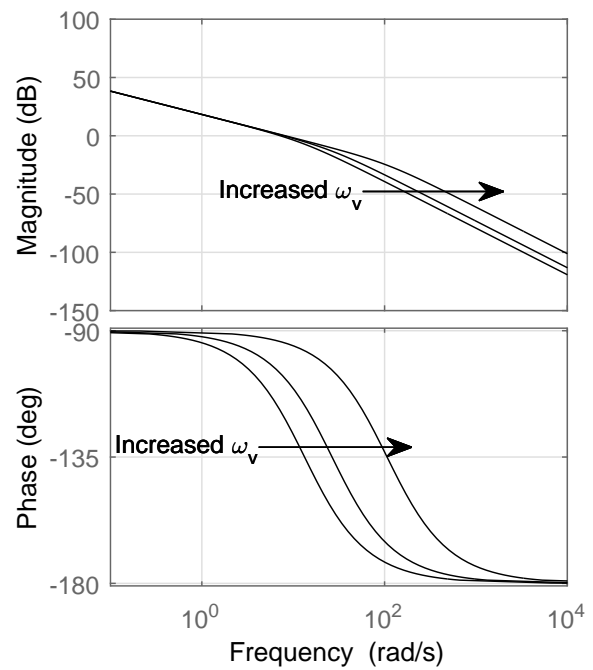
(a) Step response with varying K_s .



(a) Step response with varying ω_v .



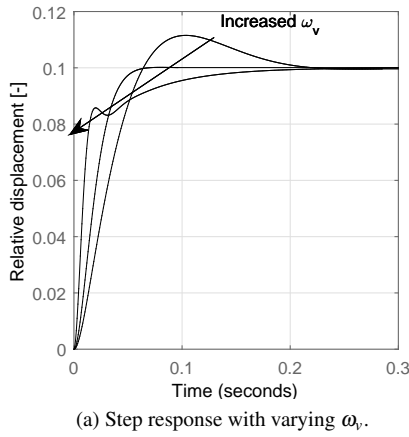
(b) Bode plot of $G_O \cdot F$ with varying K_s .



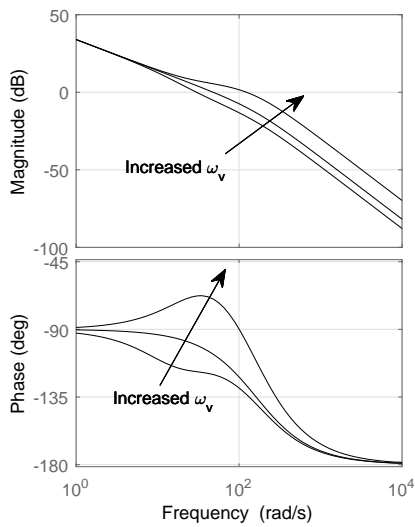
(b) Bode plot of $G_O \cdot F$ with varying ω_v .

Figure 5: Changes in system behaviour due to changes in system gain if a P-controller is used. K_s is scaled with a factor of 0.5, 1.0 and 4.0 with respect to K_{s0} .

Figure 6: Changes in system behaviour due to changes in valve break frequency if a P-controller is used. ω_v has been scaled with a factor of 0.5, 1.0 and 4.0 with respect to ω_{v0} .



(a) Step response with varying ω_v .



(b) Bode plot of $G_O \cdot F$ with varying ω_v .

Figure 7: Changes in system behaviour due to changes in valve break frequency if a P-lead-controller is used. ω_v has been scaled with a factor of 0.5, 1.0 and 4.0 with respect to ω_{v0} .

the control piston chamber, $p_{1,0}$. $p_{1,0}$ is a consequence of the force equilibrium of the swash plate mechanism.

The variation in K_q is shown in fig. 8. As can be seen, there is a difference in flow gain depending on the direction of the valve displacement. This difference is mainly a consequence of the area ratio of the control piston and the counter-acting piston (see fig. 2). The flow gain also changes with shaft speed because of the speed-dependent self-adjusting torque. The parameter with greatest impact on K_q , however, is the system pressure. From fig. 8 it may be concluded that the highest value of K_q is approximately 3 times its smallest value. If other uncertainties are taken into account, a change in system gain of maximum a factor 4 is considered reasonable.

ω_v has been observed to be relatively constant, where ap-

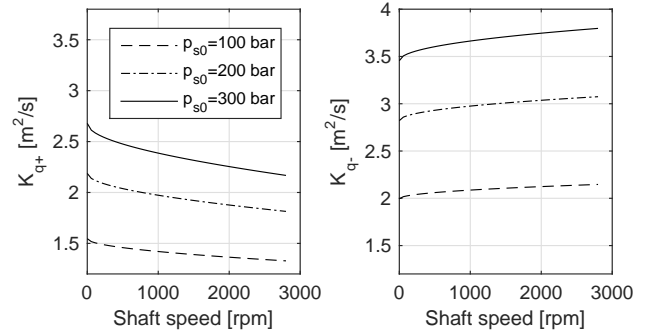


Figure 8: Variation in flow gain, K_q , for different system pressures. K_{q+} (left) is the flow gain for positive displacement of the valve, and K_{q-} (right) is the flow gain for negative displacement of the valve. The graphs were generated with eq. (3).

proximately 50 % is considered a conservative number for changes.

Since both system pressure and shaft speed are measured, gain-scheduling could be used if predictable behaviour is desired at more operating points. This approach is outside the scope of this paper, but may be considered in future work.

4.2.2 Hardware Limitations

In a linear system, it appears that ω_a and/or δ_a may be chosen arbitrarily. In a real system, however, some limitations in the hardware does not allow for this. One limitation of high significance is saturation in input signal. Here, the maximum stroke of the valve limits the maximum flow to the control piston. Also, the limitation in voltage to the solenoid tends to give over-damped responses. For the control design, this means that the choice of ω_a is limited, as too high a value would demand too high input signals.

Another issue that comes with a sampled system is noise. In particular, this concerns the P-lead-controller, due to its derivative element. For the controller design, this limits both the choice of ω_a and δ_a , as may be seen in (11). If very high δ_a and ω_a are desired, ω_2 will be very high, and the lead-compensator turns into a high-pass filter which is very sensitive to noise.

4.2.3 Summary

To summarise, changes in the values of the system gain and valve break frequency do not allow the chosen ω_a and δ_a to be achieved at all operating points with the simple model used. Rather, the introduction of the two parameters allows the controller to be trimmed in a simple and intuitive way. In particular, the parametrisation of the P-lead-controller is simplified, as the resonance and damping are directly tuned instead of gain and filter frequencies. However, the achievable values of ω_a and δ_a are ultimately limited by the maximum stroke of the valve and the hardware's sensitivity to noise.

5 Hardware Tests

To study the performance of the controllers, tests were carried out on an A11VO pump in a test rig. The test rig is briefly presented in the following subsection, while the specific test set-up and configuration which was used for the results are described in section 5.2. See [13] for more details concerning the test rig.

5.1 Test Rig

The principle of operation of the Hardware-in-the-loop (HWIL)-simulation test rig is illustrated in fig. 9. Two A11VO units are connected in an open circuit with two 20-litre Hydac accumulators. The shaft of each A11VO unit is connected to a servo-valve-controlled pump/motor which is used to simulate the surroundings of the hydraulic circuit, by either torque or speed control. The rig is thereby a typical set-up for testing of a secondary controlled transmission. In a typical use case, HWIL-simulation of a vehicle with transmission and engine is carried out. Flywheels are mounted on the shafts to lower the impact of disturbances on the speed control and to simulate engine and vehicle inertia.

The input and output signals to the hardware are handled by a data acquisition system with hardware from National Instruments (NI). During the tests, the calculations are carried out by an NI PXI-8110-RT computer that runs LabView™ in real-time with a sampling frequency of 1 kHz. Controllers and models are compiled Simulink models that are uploaded onto the PXI computer. The during-test communication with the PXI computer is handled via an Ethernet interface and a graphical user interface (GUI) on a PC.

In this paper, the displacement controller is the subject of interest. Therefore, although suitable for HWIL-simulations of secondary controlled transmissions, the rig controllers are used to maintain constant speeds of the shafts as described in the following section.

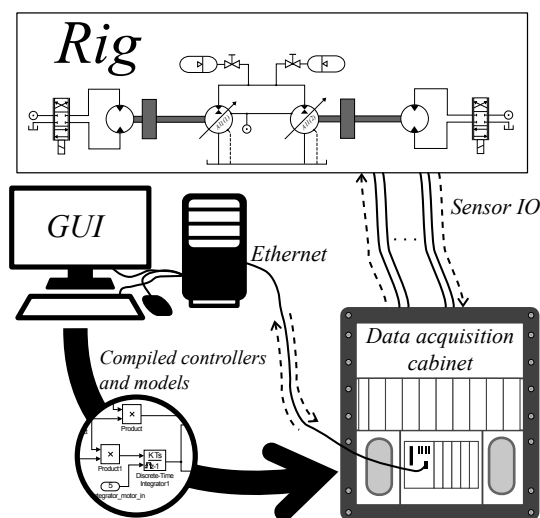


Figure 9: Principle of operation of the hardware-in-the-loop simulation rig used in the tests.

5.2 Test Set-up

Figure 10 shows the set-up that was used in the tests. The shaft of each A11VO unit was controlled at constant speed. Unit 1 was controlled at 1800 rpm and unit 2 at 1000 rpm. A pressure controller was implemented on unit 1 to control the pressure in the circuit. Unit 2 was then the subject of testing, in terms of different controllers (F) implemented in the software. The signal sent to the A11VO units was the duty cycle of the PWM signals with a PWM frequency of 200 Hz and PWM voltage of 24V. All tests were carried out at the operating temperature of the oil (approximately 40°C) and warm solenoids of the displacement actuators. Due to slow drift of the solenoid, because of temperature changes, a very small integrating element was used with the controllers. This element had very slow dynamics, and had a negligible contribution (less than 1%) to the signal in the dynamic tests that were conducted.

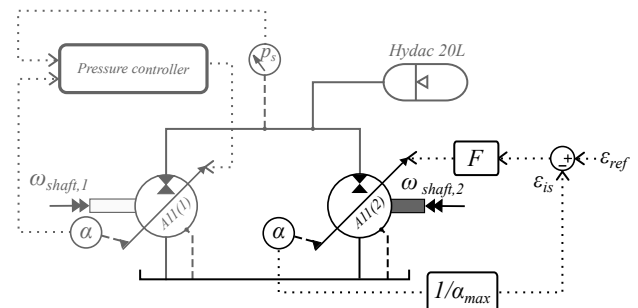


Figure 10: Set-up used in the tests.

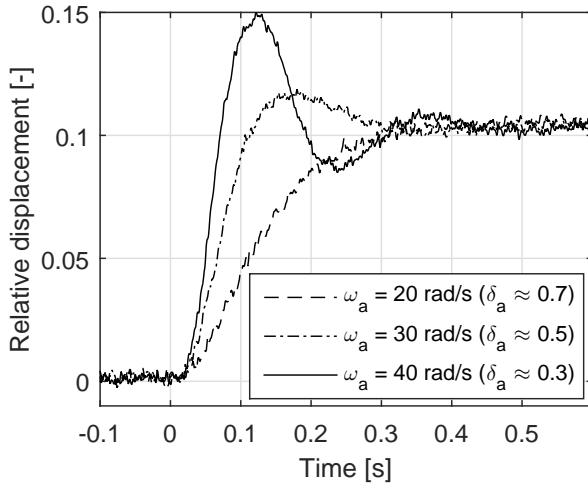
Since neither the pressure controller nor the speed controllers were completely stiff, changes in displacement on unit 2 introduced dynamic disturbances in both the system pressure and the shaft speed of unit 2. Due to the high inertia of the flywheel and the high capacitance of the accumulator, these disturbances were, however, very slow and had negligible effect on the results.

5.3 Test Cases

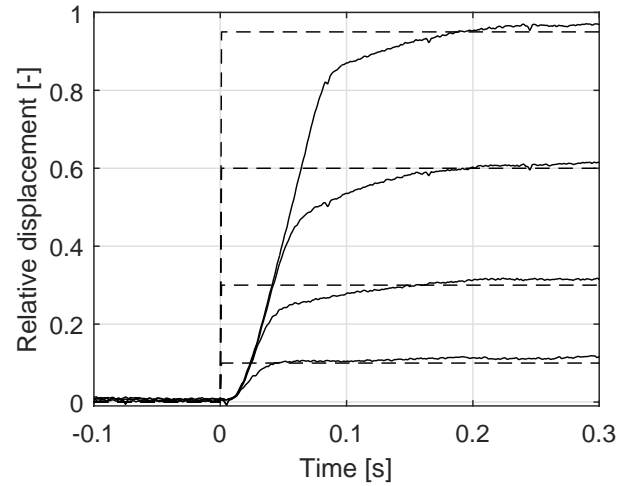
The P- and P-lead-controllers were tested at 100 bar and 1000 rpm with different values of ω_a and δ_a to study the difference in performance of the two controllers and the functionality of the pole-placement approach. The tests consisted of step responses in ϵ from 0 to 0.1.

The P-lead-controller was also tested with larger steps at system pressures of 100 bar, 200 bar and 300 bar. The purpose of these tests was to study the influence of the limitations in valve input signals on system behaviour. The time constant, i.e. the elapsed time from 0 to 63% of the step size, was measured for these steps as a comparable measure of performance.

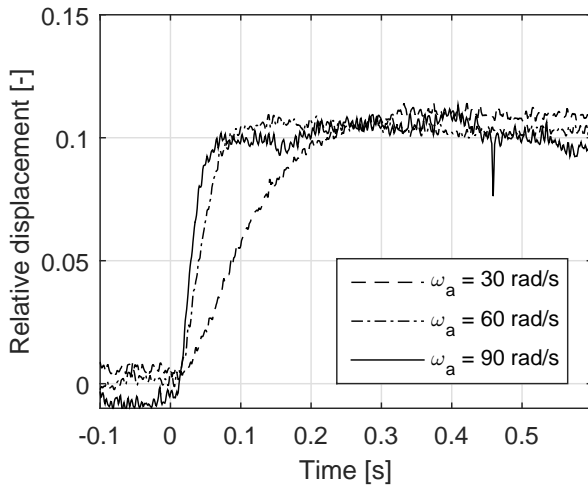
The P-controller was designed with a desired ω_a as input, i.e. with eq. (7). For both controllers, $\omega_p = 26.6$ rad/s and $K_s = 0.76$ were used. These values correspond to a shaft speed of 1000 rpm and a system pressure of 100 bar, if $K_q = K_{q-} > K_{q+}$ (see fig. 8) is used for conservative reasons.



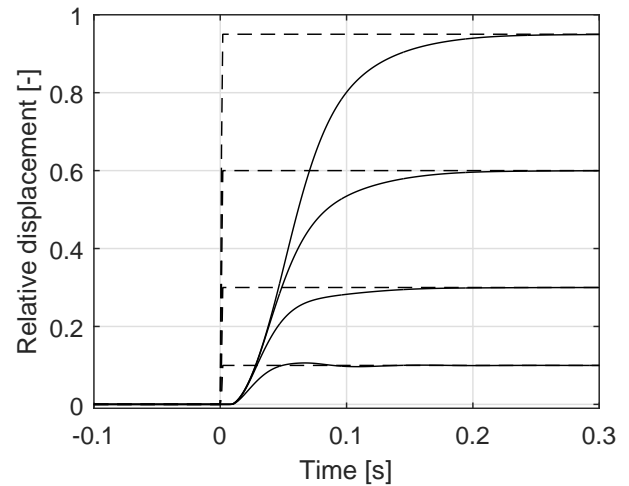
(a) P-controller.



(a) Rig measurements.



(b) P-lead-controller with $\delta_a = 0.8$.



(b) Hopsan simulations.

Figure 11: Measured step responses with different values of ω_a with P-controller (a) and P-lead-controller (b).

Figure 12: Measured (a) and simulated (b) step responses at 200 bar with $\omega_a = 90$ rad/s, and $\delta_a = 0.9$ with a P-lead-controller.

6 Results

Figure 11 shows step responses with the P-controller and the P-lead-controller for different choices of ω_a . As can be seen, an increase in desired response causes a decrease in damping with the P-controller. In contrast, the response of the P-lead-controller may be increased with a constant damping. The P-lead-controller manages responses with $\omega_a = 90$ rad/s with a relative damping of $\delta_a = 0.8$ while the P-controller is limited to $\omega_a = 20$ rad/s for approximately the same damping.

Figure 12 shows larger step responses at 200 bar with a P-lead-controller. Figure 12a displays rig measurements while fig. 12b shows the corresponding simulated results. Due to the relatively high δ_a (0.9), the responses are still reasonably damped, even though the pressure is 200 bar (the controller was parametrised for 100 bar). Furthermore, two non-linear effects may be observed. First, the limitation in valve stroke causes constant velocity in the larger steps. Second,

the voltage limitation gives extra damping at the end of the large steps. Although slightly different, the same general behaviour is present in both the model and the measurements, which should indicate that the model captures the relevant non-linearities.

Table 1 shows the measured time constants for different step sizes and system pressures. It is clear that the displacement controller becomes slower as the step size increases, which is due to the limitations in voltage and valve stroke. For step sizes below 0.3, the pressure has little effect on the response. For larger steps on the other hand, increased pressure decreases the time constant primarily because of the maximum deliverable flow of the valve that increases with the pressure.

Table 1: Measured time constants (0→63%) in milliseconds for different step sizes and different pressures. The same controller as the one used for the results in fig. 12 was used in all cases.

↓Step size, System Pressure [bar]→	100	200	300
0.1	26	25	29
0.3	39	36	38
0.6	56	49	49
0.95	81	64	60

7 Discussion

The performance of the P-lead-controller is superior to that of the P-controller in terms of fast response with high relative damping. This is because the valve response is rather slow and therefore limits the closed-loop response with the P-controller. On the other hand, the P-lead-controller can cancel out the valve dynamics and thereby increase the response significantly. For small steps, the P-lead-controller was able to produce a response with approximately 4 times higher resonance than the P-controller, with the same relative damping.

Although high, the performance of the P-lead-controller is limited for large steps. One reason for this phenomenon is the limitation in solenoid voltage. The behaviour is similar to the case when the valve is slightly faster than the controller assumes (see fig. 7a, sec. 4.2.1), and in simulations it has been found that the effect could be lowered if ω_1 is chosen as slightly higher than ω_v .

Another reason for deteriorated performance for large steps is the limited flow of the valve, a finding consistent with previous work [10]. In that particular study, however, a 4-way servo-valve with external pressure supply was used, and there was therefore no increased response at increased system pressures. With a 3-way valve configuration, in early studies the controller was found to be sensitive to system pressure fluctuations and inherently less stable [9]. This has not been a problem in the system studied in this paper, due to the inclusion of a high-capacitance accumulator in the circuit. However, if a similar concept is to be used in a system with low capacitance, dependencies of system pressure fluctuations should probably be considered.

The influence of the self-adjusting torque that acts on the swash plate has only been considered in terms of its mean value. In reality, this torque oscillates with a frequency that is proportional to the shaft speed. Therefore, in previous research it has been pointed out that this should be considered in the controller design [16]. In fact, it has been found that for the floating cup pump, oscillations of the swash plate have a negative impact on pump efficiency [17]. However, oscillations of the swash plate due to the self-adjusting torque seem to be machine-dependent, and have not yet been observed in the A11VO units studied in this paper.

As seen from the results, the pole placement approach may be used to produce a predictive response of the displacement controller. In turn, this ability relies on an accurate

model as input when the controller is parametrised. The behaviour will therefore change due to model uncertainties as well as hardware limitations and operation-point-dependent parameter variations. In the studied system, however, the dominance of low-order dynamic properties in the system makes it rather robust against instability caused by changes in parameter values. Thus, the main benefit of the pole placement approach identified in this paper is its simple implementation rather than predictable behaviour. Should predictable behaviour of the displacement controller at more operating points be highly desirable, gain scheduling of the system pressure could be a beneficial extension of the control concept. It should be mentioned, however, that the pressure has not been found to have as high influence on system gain in the measurements as it has in the simulations. The valve behaviour also has a high impact on the response, which suggests that an enhanced valve model could be useful. For example, the solenoid is sensitive to temperature changes. This effect could be lowered if current control was implemented rather than voltage control. It is important to note, however, that the response for large steps is primarily limited by the maximum flow of the valve.

8 Conclusions

To conclude, the pole-placement approach used in this paper allows the displacement controller to be designed in a simple way as long as an accurate system model is available. In particular, the proportional-lead control concept is promising as it allows more than 4 times as high resonance compared to the proportional-control concept with the same relative damping. In step responses, time constants (0→63% of final value) from 26 ms to 81 ms have been measured in hardware tests. The time constant tends to increase with system pressure and decrease with step size, due to the maximum flow of the control valve.

The realisation of heavy hydraulic hybrid construction machines relies on secondary control and thereby also on fast displacement controllers. The results reported in this paper will therefore be useful input in further research on full-vehicle control of such machines.

9 Acknowledgements

This research was partially funded by the Swedish Energy Agency (Energimyndigheten). The authors also wish to thank Bosch Rexroth for providing the prototype pumps.

References

- [1] Lino Guzella and Antonio Sciarretta. *Vehicle Propulsion Systems*. Springer Verlag Berlin Heidelberg, 2013.
- [2] A. Pourmovahed. Vehicle propulsion systems with hydraulic energy storage: a literature survey. *International Journal of Vehicle Design*, 12(4):378–403, 1991.
- [3] Karl-Erik Rydberg. Energy Efficient Hydraulic Hybrid Drives. In *The 11:th Scandinavian International Conference on Fluid Power, SICFP'09*, Linköping, Sweden, 2009.

- [4] Rolf Kordak. *Hydrostatic drives with secondary control*. Mannesmann Rexroth GmbH, 1996.
- [5] Göran Palmgren. *On Secondary Controlled Hydraulic Systems*. Licentiate thesis, Linköping University, 1988.
- [6] H Berg and M Ivantysynova. Design and testing of a robust linear controller for secondary controlled hydraulic drive. *Proceedings of the Institution of Mechanical Engineers, Part I: Journal of Systems and Control Engineering*, 213(5):375–386, 1999.
- [7] L Viktor Larsson, Karl Pettersson, and Petter Krus. Mode Shifting in Hybrid Hydromechanical Transmissions. In *Proceedings of the ASME/BATH 2015 Symposium on Fluid Power and Motion Control (FPMC2015)*, Chicago, Illinois, USA, 2015.
- [8] Jaroslav Ivantysyn and Monika Ivantysynova. *Hydrostatic Pumps and Motors*. Akademia Books International, New Delhi, India, 2001.
- [9] W.L. Green and T.R. Crossley. An Analysis of the Control Mechanism used in Variable-Delivery Hydraulic Pumps. In *Proceedings of the Institution of Mechanical Engineers*, 1970.
- [10] Joerg Grabbel and Monika Ivantysynova. An investigation of swash plate control concepts for displacement controlled actuators. *International Journal of Fluid Power*, 6(2):19–36, 2005.
- [11] Noah D. Manring. *Fluid Power Pumps & Motors*. McGraw-Hill Education, 2013.
- [12] Herbert E Merritt. *Hydraulic Control Systems*. John Wiley & Sons, Inc., 1967.
- [13] L. Viktor Larsson and Petter Krus. Modelling of the Swash Plate Control Actuator in an Axial Piston Pump for a Hardware-in-the-Loop Simulation Test Rig. In *9th FPNI Ph.D. Symposium on Fluid Power*, Florianópolis, SC, Brazil, 2016.
- [14] <http://www.iei.liu.se/flumes/system-simulation/hopsann/>. Division of Fluid and Mechatronic Systems, Linköping University, Accessed: 2017-04-11.
- [15] Torkel Glad and Lennart Ljung. *Reglerteknik: Grundläggande teori*. Studentlitteratur AB, 2006.
- [16] Liselott Ericson. Swash Plate Oscillations due to Piston Forces in Variable In-line Pumps. In *The 9th International Fluid Power Conference, (9. IFK)*, Aachen, Germany, 2014.
- [17] P. a. J. Achten, S Eggenkamp, and H. W. Potma. Swash plate oscillation in a variable displacement floating cup pump. In *The 13th Scandinavian International Conference on Fluid Power*, pages 163–176, Linköping, Sweden, 2013.

A Nomenclature

Designation	Denotation	Unit
A_1	Control piston area	m ²
α	Swash plate angle	radians
C_q	Valve flow coefficient	-
d	Valve spool diameter	m
δ_a	Desired relative damping	-
ε	Relative displacement (V/V_{max})	-
F	Controller transfer function	-
G_C	Closed loop transfer function	-
G_O	Open loop transfer function	-
k_{PWM}	Static solenoid gain	m/%Duty cycle
K	Controller gain	1/%Duty cycle
K_q	Valve flow gain	m ² /s
K_s	Static system gain	1/%Duty-cycle
L	Control piston lever	m
$\omega_{1,2}$	Controller break frequency	rads/sec
ω_a	Desired resonance frequency	rads/sec
ω_{shaft}	Shaft angular velocity	rads/sec
ω_v	Valve break frequency	rads/sec
p_1	Control piston pressure	Pa
p_b	Boost pressure	Pa
p_s	System pressure	Pa
p_T	Tank pressure	Pa
q	Volumetric flow	m ³ /s
ρ	Oil density	kg/m ³
u_{PWM}	Pulse-width-modulated voltage	% Duty-cycle
V	Displacement volume	m ³ /rad
x_v	Valve displacement	m